

# What is chiral susceptibility probing?



Hidenori Fukaya (Osaka U.)

for JLQCD collaboration

[S. Aoki, Y. Aoki, HF, S. Hashimoto, I.Kanamori,

T. Kaneko, Y. Nakamura, C. Rohrhofer and K. Suzuki ]

S. Aoki, Y. Aoki, HF, S. Hashimoto, C. Rohrhofer, K. Suzuki,

PTEP 2022 (2022) 2, 023B05 [[2103.05954](#)] [hep-lat]

(and preliminary results in  $N_f=2+1$  simulations)

# Acknowledgments

Resources:

- **Fugaku** (hp200130, hp210165, hp210231)

- **Oakforest-PACS [JCAHPC]**

HPCL projects : hp170061, hp180061, hp190090, hp200086, hp210104,

MCRP in CCS, U. Tsukuba : xg17i032 and xg18i023

- Wisteria/BDEC-01 [HPCL: hp220093, MCRP: wo22i038]

- Polarie/Grand Chariot (hp200130)

- Flow

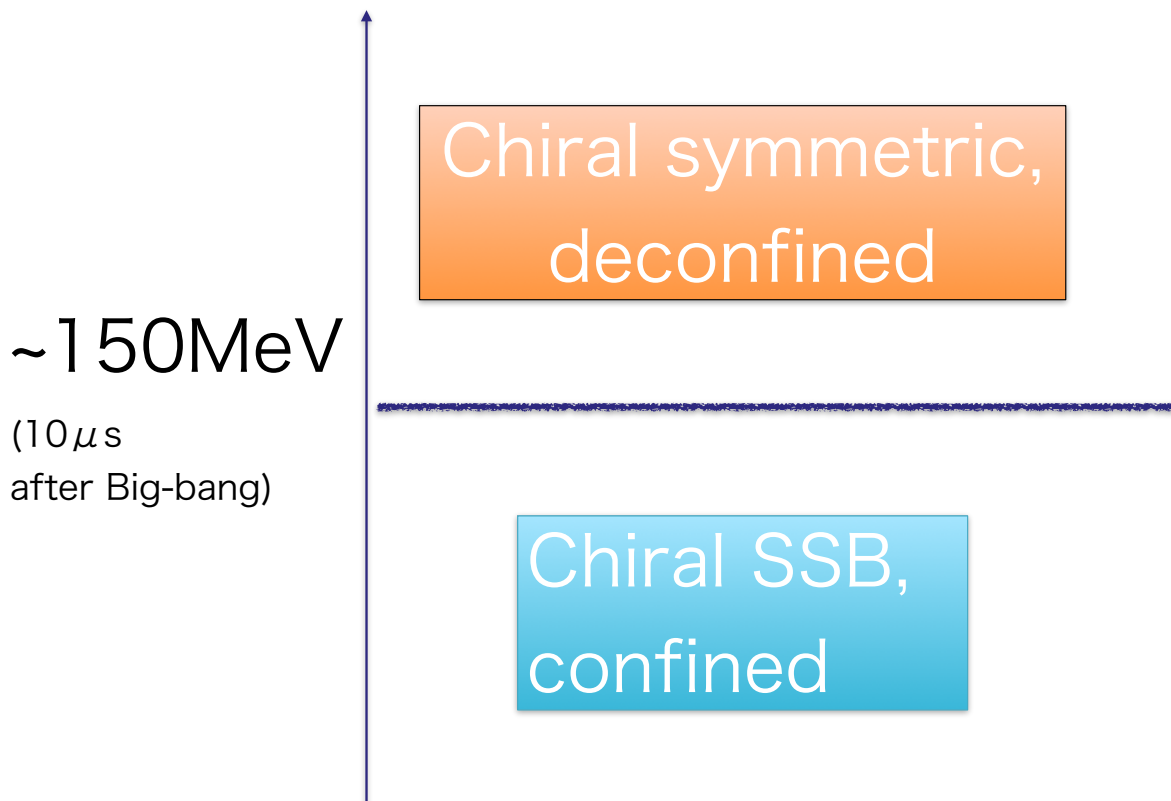
- SQUID

- Program for Promoting Researches on the Supercomputer Fugaku, Simulation for basic science: from fundamental laws of particles to creation of nuclei Joint

- Institute for Computational Fundamental Science (JICFuS)

# QCD phase transition

Temperature



Chiral condensate (at  $m=0$ )  
probes  $SU(2)_L \times SU(2)_R$   
symmetry breaking/  
restoration :

$$\text{For } T > T_c, \quad \langle \bar{q}q \rangle = 0$$

$$\text{For } T < T_c, \quad \langle \bar{q}q \rangle \neq 0$$

# Chiral susceptibility

QCD partition function

$A$  : gluon fields

$$Z(m) = \int [dA] \det(D(A) + m)^{N_f} e^{-S_G(A)}$$

chiral condensate

$$-\langle \bar{q}q \rangle = \frac{1}{N_f V} \frac{\partial}{\partial m} \ln Z(m)$$

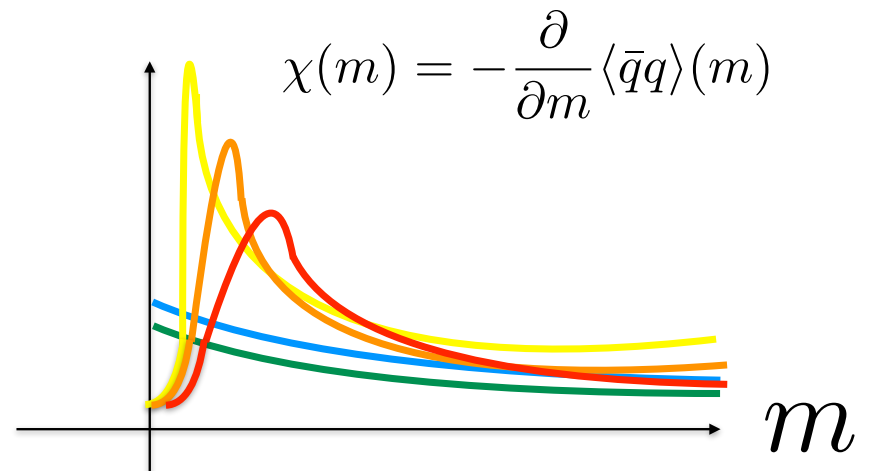
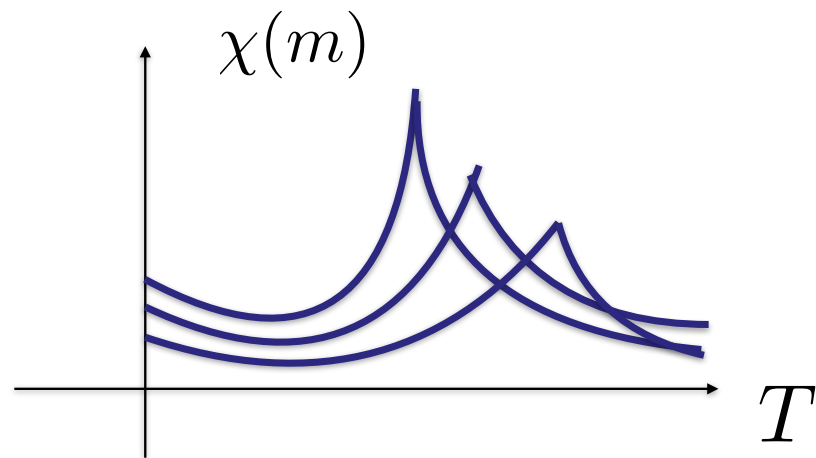
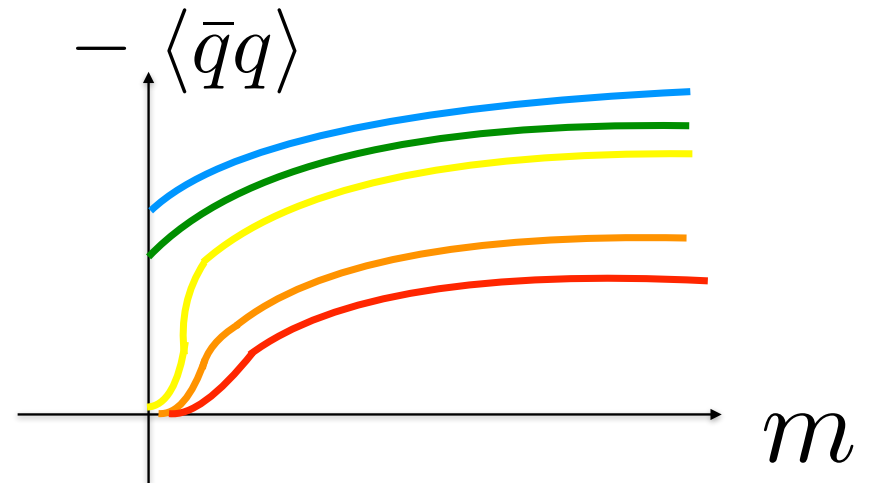
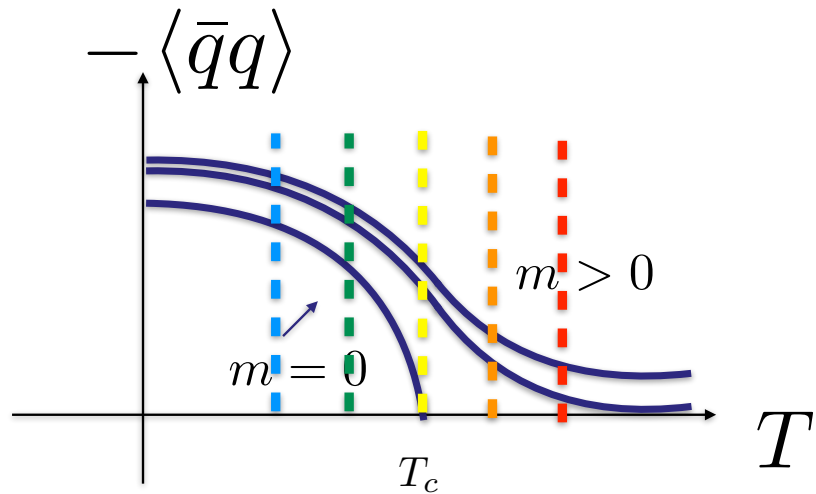
chiral susceptibility

$$\chi(m) = -\frac{\partial}{\partial m} \langle \bar{q}q \rangle(m)$$

In this talk,  $N_f = 2$  ( $m_u = m_d = m$ )

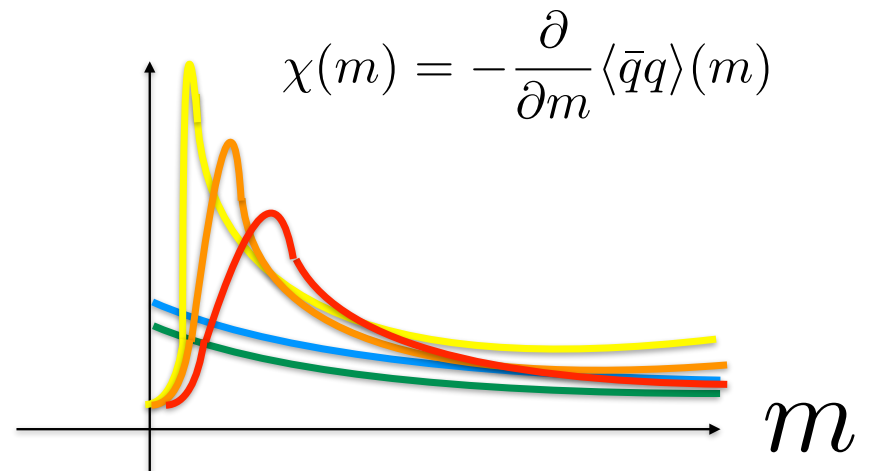
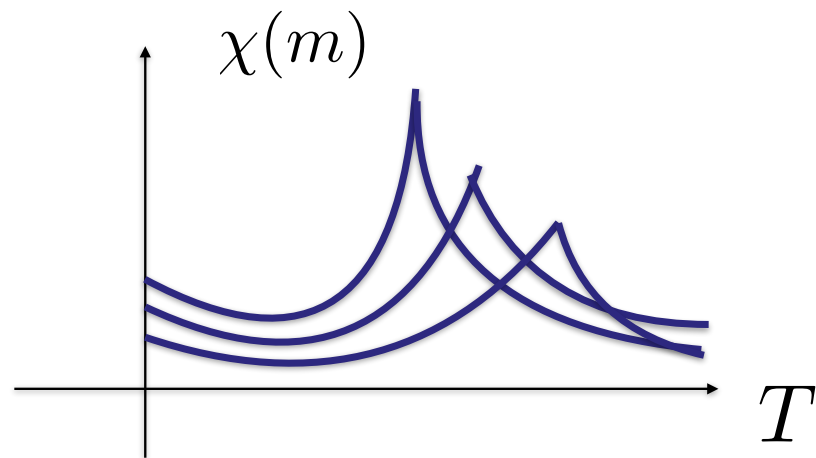
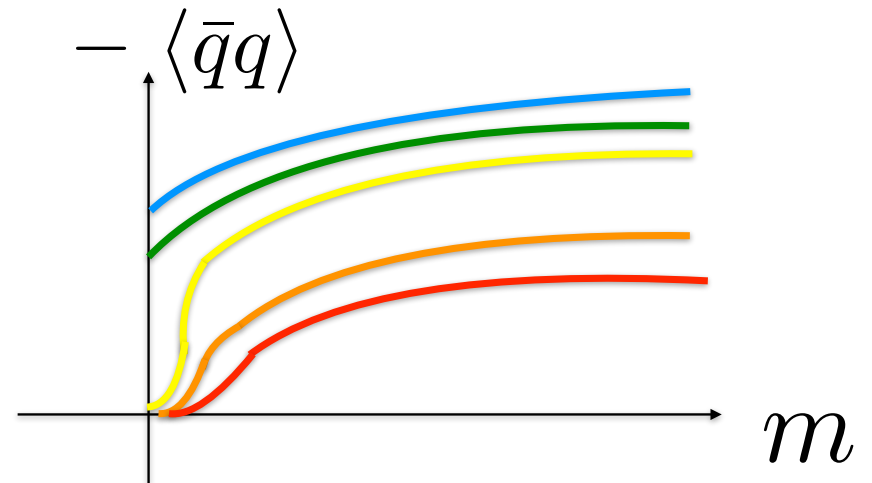
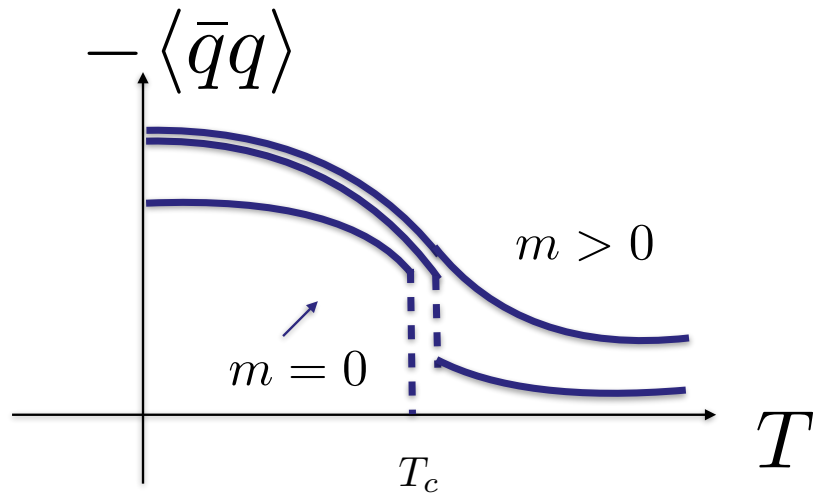
\* strange quark is just a spectator.

# Temperature(T) and mass(m) dependence



# When the transition is 1st order

\* But finite  $V$  effect makes the transition not sharp.



# Chiral phase transition

Chiral condensate probes

$SU(2)_L \times SU(2)_R$  symmetry breaking/restoration :

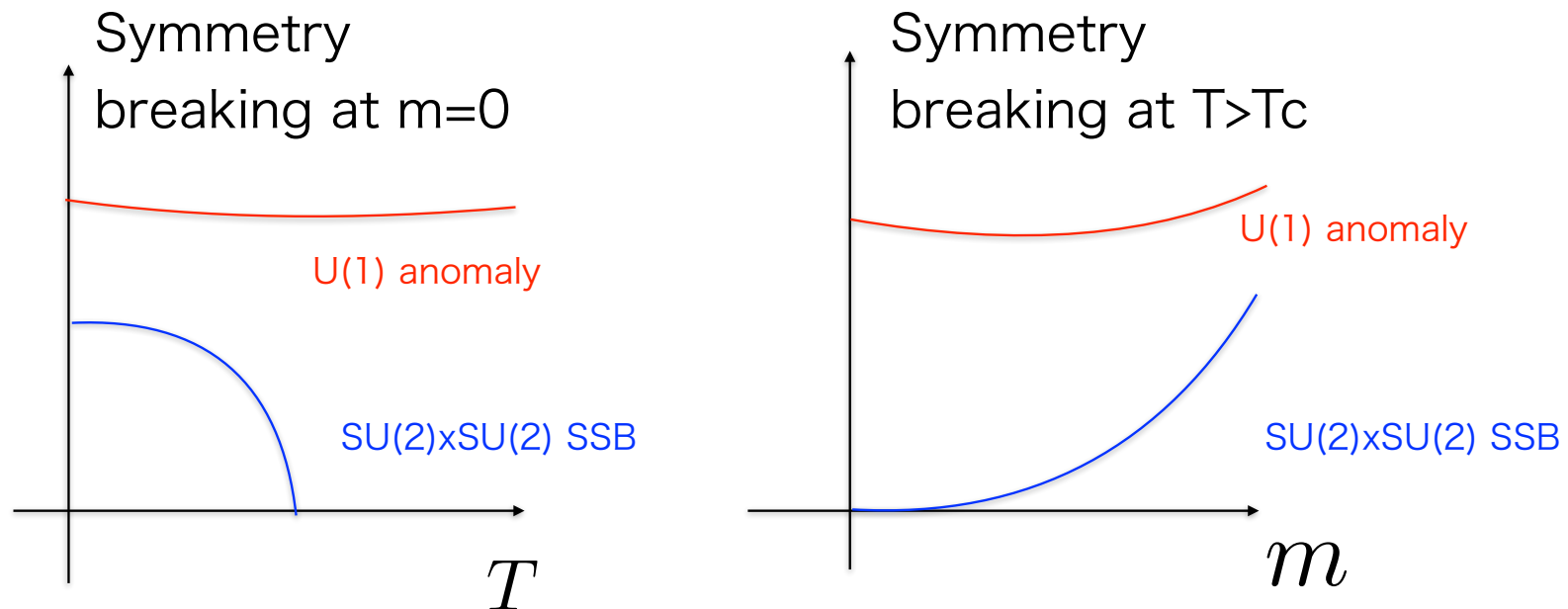
For  $T < T_c$ ,  $\langle \bar{q}q \rangle \neq 0$       For  $T > T_c$ ,  $\langle \bar{q}q \rangle = 0$

But  $\langle \bar{q}q \rangle$  also breaks  $U(1)_A$  symmetry.

Question:

How much does  $U(1)_A$  (anomaly) contribute to the transition?

# Naive expectation: U(1) anomaly exists at any energy scale (does not change much)



You may think that  $T$  and  $m$  dependences of chiral condensate should reflect  $SU(2)_L \times SU(2)_R$  breaking rather than U(1) anomaly.



## But in early days of QCD

QCD founders in 70's and 80's thought

instanton  $\rightarrow$  axial U(1) anomaly  $\rightarrow$  SU(2)xSU(2) breaking.

Callan, Dashen & Gross 1978:

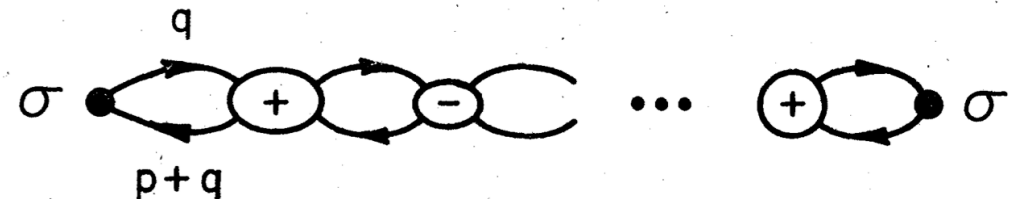


FIG. 9. The structure of the diagrams that produce a tachyon in the  $\sigma$  channel. The + (-) blobs refer to the effective determinantal four-fermion interaction induced by instantons (anti-instantons).

If this inverse is true, we should have

instanton disappears  $\rightarrow$  anomaly disappears  $\rightarrow$  SU(2)xSU(2) restored.

# It has been difficult issue.

Analytic method:

Semi-classical QCD instantons are not enough to describe the low-energy dynamics of QCD.

Lattice simulations :

Staggered fermions explicitly breaks

$$SU(2)_L \times SU(2)_R \times U(1)_A \rightarrow U(1)_A,$$

Wilson fermion explicitly breaks

$$SU(2)_L \times SU(2)_R \times U(1)_A \rightarrow SU(2)_V$$

Moreover, we found that

**lattice artifacts are enhanced at high temperature**

(even for domain-wall fermions)

[JLQCD 2015, 2016]

## Our work

In this work we study chiral condensate and its susceptibility in 2- and 2+1-flavor QCD

with exactly chiral symmetric Dirac operator.

We separate the axial U(1) breaking (in particular topological ) effect from others in a clean way.

Our result shows that

signal of chiral susceptibility is dominated by axial U(1) breaking effect (at  $T \geq T_c$ ),

rather than  $SU(2)_L \times SU(2)_R$ .

# Contents

## ✓ 1. Introduction

We simulate the chiral phase transition of  $N_f=2$  QCD with chiral fermions to investigate the role of axial  $U(1)$  anomaly.

## 2. $U(1)_A$ contribution to chiral susceptibility

## 3. Numerical results

## 4. Summary

# Dirac eigenmode decomposition

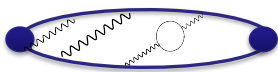
$$Z(m) = \int [dA] \det(D(A) + m)^{N_f} e^{-S_G(A)} = \int [dA] \prod_{\lambda} (i\lambda(A) + m)^{N_f} e^{-S_G(A)}$$

O(100) eigenvalues can be computed on the lattice.

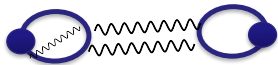
$$-\langle \bar{q}q \rangle = \frac{1}{N_f V} \frac{\partial}{\partial m} \ln Z(m) = \frac{1}{V} \left\langle \sum_{\lambda} \frac{1}{i\lambda(A) + m} \right\rangle,$$

chiral susceptibility

$$\chi(m) = \frac{1}{N_f V} \frac{\partial^2}{\partial m^2} \ln Z(m) = \chi^{con.}(m) + \chi^{dis.}(m),$$

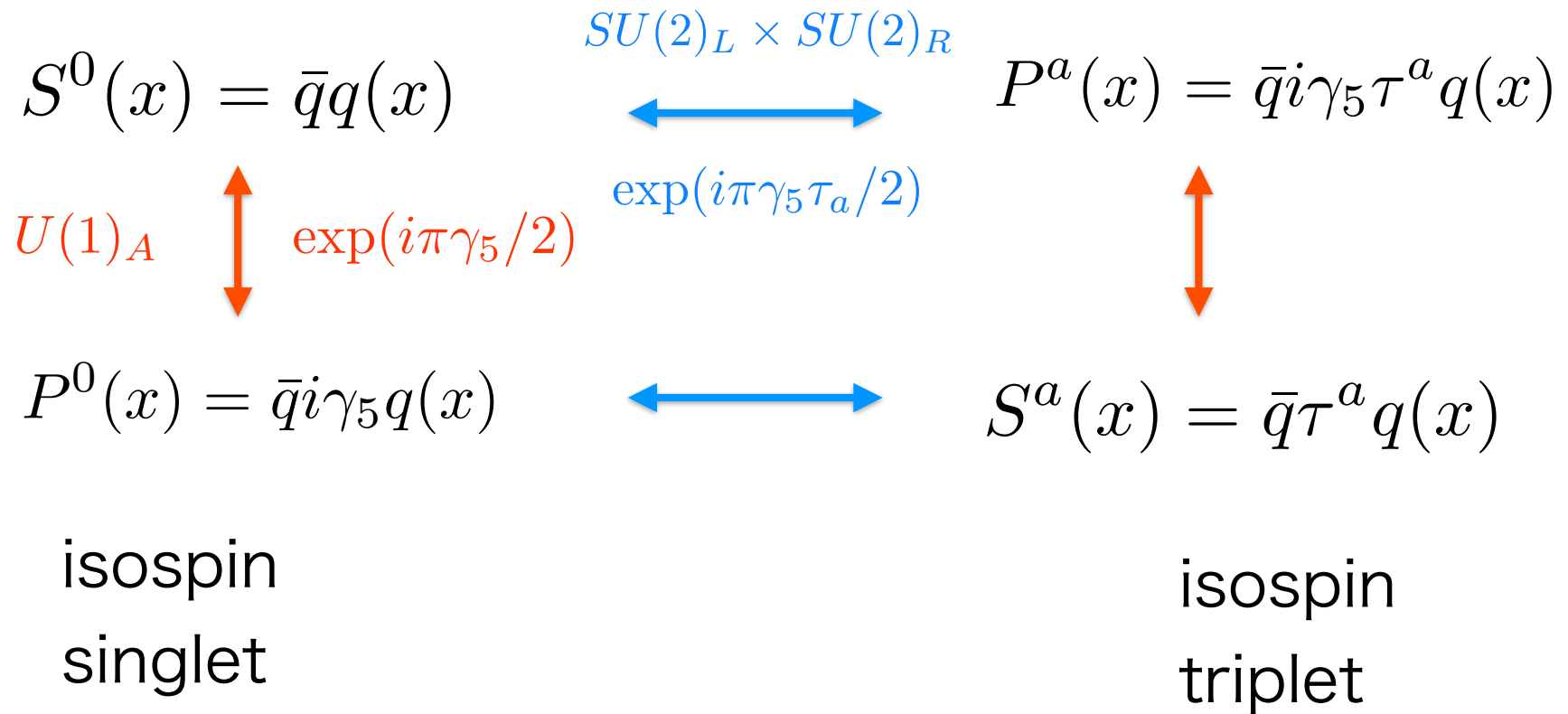
$$\chi^{con.}(m) = - \frac{\partial}{\partial m_{valence}} \langle \bar{q}q \rangle \Big|_{m_{valence}=m}$$


The diagram shows a blue oval representing a valence quark loop. It has two blue dots at the ends, representing quark and antiquark vertices. Inside the oval, there are two wavy lines representing gluon exchanges between the vertices.

$$\chi^{dis.}(m) = - \frac{\partial}{\partial m_{sea}} \langle \bar{q}q \rangle \Big|_{m_{sea}=m}$$


The diagram shows a sea quark loop. It consists of two blue circles, each with a blue dot, representing quark and antiquark vertices. These vertices are connected by two wavy lines representing gluon exchanges. The entire structure is enclosed in a larger blue oval.

# Chiral rotations (with angle $\pi$ )



# Relation to scalar susceptibility

$$L_{\text{QCD}} = \left[ \frac{1}{4} \text{Tr} F_{\mu\nu} F^{\mu\nu} + \bar{q} (\gamma^\mu (\partial_\mu - igA_\mu) + m) q \right]$$

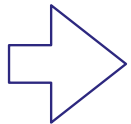
$$\chi(m) = \frac{1}{N_f V} \frac{\partial^2}{\partial m^2} \ln Z(m, \theta = 0)$$

$$= - \sum_x \langle S^0(x) S^0(0) \rangle - V \langle S^0 \rangle^2 \qquad S^0(x) = \bar{q} q(x)$$

# Relation to pseudoscalar susceptibility

$$\begin{aligned} Z(m, \theta) &= \int [dA] \det(D(A) + m)^{N_f} e^{-S_G(A) + i\theta Q(A)} \\ &= \int [dA] \det(D(A) + m e^{i\gamma_5 \theta / N_f})^{N_f} e^{-S_G(A)} \quad \leftarrow \text{U(1)}_A \text{ rotation} \end{aligned}$$

$$\chi_{\text{top.}}(m) = -\frac{1}{N_f V} \frac{\partial^2}{\partial \theta^2} \ln Z(m, \theta) \Big|_{\theta=0} = m \left[ \frac{\partial}{\partial \theta} \langle \bar{q} i \gamma_5 e^{i\gamma_5 \theta / N_f} q \rangle \right] \Big|_{\theta=0}$$

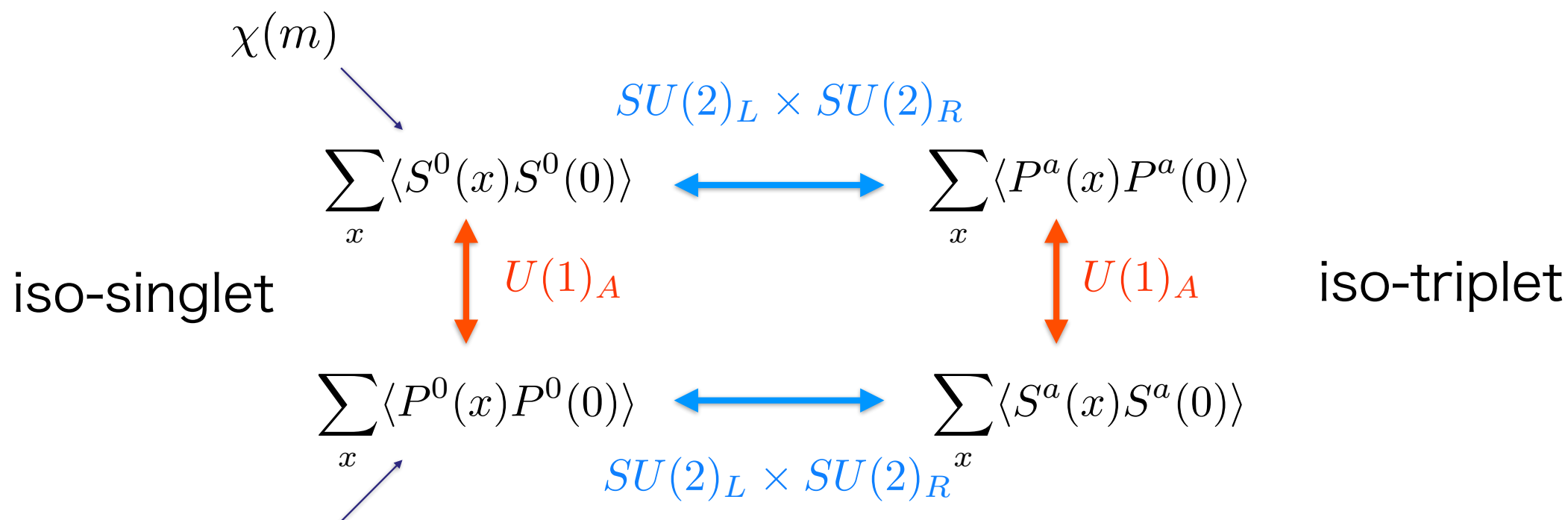


$$\frac{N_f}{m^2} \chi_{\text{top.}}(m) = - \sum_x \langle P^0(x) P^0(0) \rangle - \frac{\langle \bar{q} q \rangle(m)}{m}. \quad P^0(x) = \bar{q} i \gamma_5 q(x)$$

\* $N_f = 2$



# Symmetry structure of scalar/pseudoscalar susceptibilities



$$-\frac{N_f}{m^2} \chi_{\text{top.}}(m) - \frac{-\langle \bar{q}q \rangle(m)}{m}$$

See also LLNL/RBC Collaboration 2014, Nicola & Elvira 2018, Nicola 2020.

# Connected/disconnected pseudoscalar susceptibilities

From a Ward-Takahashi identity  $0 = \langle \delta_{SU(2)}^a P^a(0) \rangle - \langle \delta_{SU(2)}^a S P^a(0) \rangle$ ,  
we have

$$m \sum_x \langle P^a(x) P^a(0) \rangle + \langle S^0 \rangle = 0.$$

Therefore,

$$\begin{aligned} \frac{N_f}{m^2} \chi_{\text{top.}}(m) &= - \sum_x \langle P^0(x) P^0(0) \rangle - \frac{\langle S(0) \rangle}{m} \\ &= \sum_x \langle P^a(x) P^a(0) \rangle - \sum_x \langle P^0(x) P^0(0) \rangle \end{aligned}$$

# Connected/disconnected scalar

# susceptibilities

$$\chi(m) = \chi^{\text{con.}}(m) + \chi^{\text{dis.}}(m)$$

$$\begin{aligned}\chi^{\text{con.}}(m) &= \sum_x \langle S^a(x) S^a(0) \rangle = \sum_x \langle S^a(x) S^a(0) - P^a(x) P^a(0) \rangle + \sum_x \langle P^a(x) P^a(0) \rangle \\ &= -\Delta_{U(1)}(m) + \frac{-\langle \bar{q} q \rangle(m)}{m}\end{aligned}$$

$$\begin{aligned}\chi^{\text{dis.}}(m) &= \sum_x \langle S^0(x) S^0(0) - S^a(x) S^a(0) \rangle - V \langle S^0(0) \rangle^2 \\ &= \sum_x \langle [S^0(x) S^0(0) - \langle S^0(0) \rangle^2 - P^a(x) P^a(0)] + [P^a(x) P^a(0) - S^a(x) S^a(0)] \rangle \\ &= \Delta_{SU(2)}^{(1)}(m) + [P^a(x) P^a(0) - P^0(x) P^0(0)] + [P^0(x) P^0(0) - S^a(x) S^a(0)] \\ &= \Delta_{SU(2)}^{(1)}(m) + \frac{N_f \chi_{\text{top.}}(m)}{m^2} - \Delta_{SU(2)}^{(2)}(m)\end{aligned}$$

# Separating U(1)<sub>A</sub> breaking part

$$\chi(m) = \chi^{\text{con.}}(m) + \chi^{\text{dis.}}(m)$$

$$\chi^{\text{con.}}(m) = \underbrace{-\Delta_{U(1)}(m) + \frac{\langle |Q(A)| \rangle}{m^2 V}}_{\text{U(1)}_A \text{ breaking contribution}} \underbrace{- \frac{-\langle \bar{q}q \rangle_{\text{sub.}}(m)}{m}}_{\text{mixed}}$$

\* quadratic divergence is subtracted using the data at reference quark mass  $m_{\text{ref}}=0.005$ .

$$\chi^{\text{dis.}}(m) = \underbrace{\frac{N_f}{m^2} \chi_{\text{top.}}(m)}_{\text{U(1)}_A \text{ breaking contribution}} + \underbrace{\Delta_{SU(2)}^{(1)}(m) - \Delta_{SU(2)}^{(2)}(m)}_{\text{SU(2)} \times \text{SU(2) breaking}}$$

SU(2) × SU(2) breaking

where  $\Delta_{U(1)}(m) \equiv \sum_x \langle P^a(x)P^a(0) - S^a(x)S^a(0) \rangle$  axial U(1) susceptibility

$$\Delta_{SU(2)}^{(1)}(m) \equiv \sum_x \langle S^0(x)S^0(0) - P^a(x)P^a(0) \rangle \quad \Delta_{SU(2)}^{(2)}(m) \equiv \sum_x \langle S^a(x)S^a(0) - P^0(x)P^0(0) \rangle$$

# Lattice formulas

Using  $\lambda_m =$  eigenvalues of  $H_m = \gamma_5[(1 - m)D_{ov} + m]$

$$\Delta_{U(1)}(m) = \frac{1}{V(1 - m^2)^2} \left\langle \sum_{\lambda_m} \frac{2m^2(1 - \lambda_m^2)^2}{\lambda_m^4} \right\rangle,$$

$$-\langle \bar{q}q \rangle = \frac{1}{V(1 - m^2)} \left\langle \sum_{\lambda_m} \frac{m(1 - \lambda_m^2)}{\lambda_m^2} \right\rangle.$$

$$\chi^{\text{dis.}}(m) = \frac{N_f}{V} \left[ \frac{1}{(1 - m^2)^2} \left\langle \left( \sum_{\lambda_m} \frac{m(1 - \lambda_m^2)}{\lambda_m^2} \right)^2 \right\rangle - |\langle \bar{q}q \rangle^{\text{lat}}|^2 V^2 \right].$$

Remark.1 eigen functions do not matter.

Remark.2 chiral symmetry is essential for this decomposition.

# Contents

## ✓ 1. Introduction

We simulate the chiral phase transition of  $N_f=2$  QCD with chiral fermions to investigate the role of axial  $U(1)$  anomaly.

## ✓ 2. $U(1)_A$ contribution to chiral susceptibility

can be separated using Ward-Takahashi identities etc.

## 3. Numerical results

## 4. Summary

# Simulation setup (Nf=2)

Nf=2 flavor QCD

$1/a = 2.6 \text{ GeV}$  (0.075fm)

Symanzik gauge action

$L=24,32,40,48$  [1.8-3.6fm] (at  $T=220\text{MeV}$ )

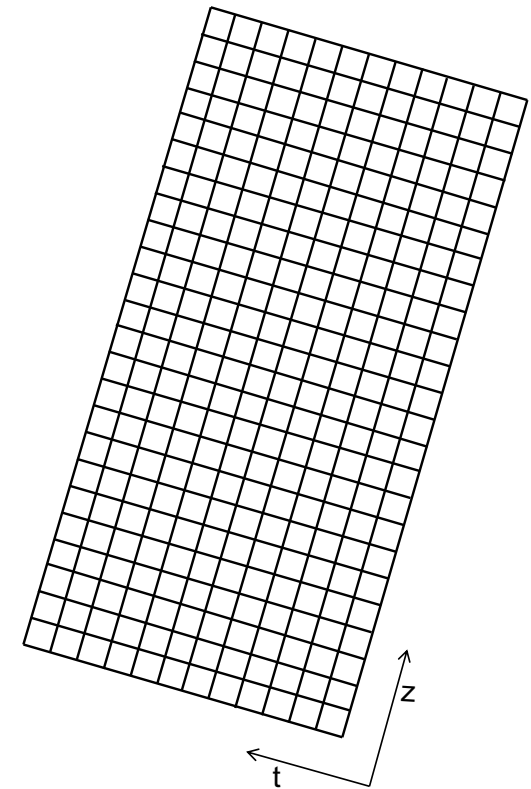
Mobius domain-wall fermions with  $m_{\text{res}} < 1 \text{ MeV}$

(and reweighted overlap fermion)

Quark mass from 3MeV (< phys. pt.  $\sim 4\text{MeV}$ ) to 30MeV.

$T=165$  ( $\sim T_c$ ), 195, 220, 260, 330 MeV ( $L_t=8,10,12,14,16$ )

$T_c$  is estimated to be around 175MeV (from Polyakov loop)



**Simulation codes : Irolro++** (<https://github.com/coppolachan/Irolro>)

**Grid** (<https://github.com/paboyle/Grid>)

# Simulation setup ( $N_f=2+1$ )

## [preliminary]

$N_f=2+1$  flavor QCD

$1/a = 2.453\text{GeV}$

$L=32$  (2.58, fm)

Mobius domain-wall fermion with  $m_{\text{res}} < 1\text{ MeV}$

(and reweighted overlap fermion)

up-down quark mass from **phys. pt.**  $\sim 4\text{ MeV}$  to  $30\text{ MeV}$ .

strange quark mass at phys.pt.

$T=153(\sim T_c), 175, 220\text{ MeV}$



# Low-mode approximation

In the eigenvalue summations,

$$\Delta_{U(1)}(m) = \frac{1}{V(1-m^2)^2} \left\langle \sum_{\lambda_m} \frac{2m^2(1-\lambda_m^2)^2}{\lambda_m^4} \right\rangle,$$

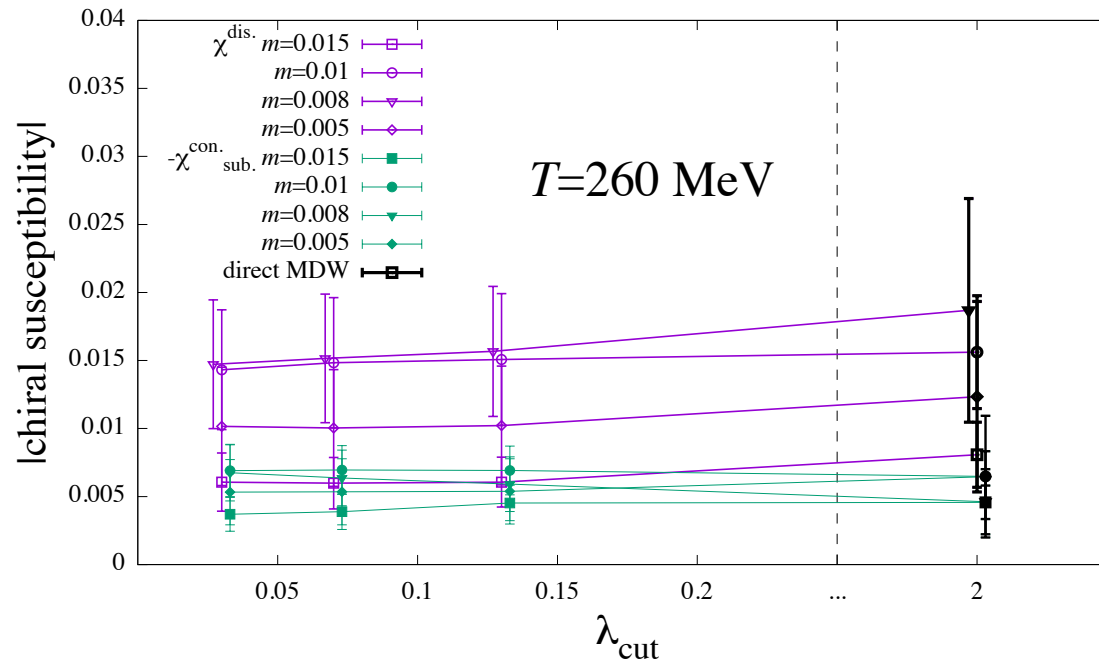
$$-\langle \bar{q}q \rangle = \frac{1}{V(1-m^2)} \left\langle \sum_{\lambda_m} \frac{m(1-\lambda_m^2)}{\lambda_m^2} \right\rangle.$$

$$\chi^{\text{dis.}}(m) = \frac{N_f}{V} \left[ \frac{1}{(1-m^2)^2} \left\langle \left( \sum_{\lambda_m} \frac{m(1-\lambda_m^2)}{\lambda_m^2} \right)^2 \right\rangle - |\langle \bar{q}q \rangle^{\text{lat}}|^2 V^2 \right].$$

where  $\lambda_m =$  eigenvalues of  $H_m = \gamma_5[(1-m)D_{ov} + m]$

we truncate at 30-40th lowest mode ( $\lambda_{\text{threshold}} \sim 150\text{--}300$  MeV).

# Low mode approximation



For  $T \leq 260$  MeV, we find a good saturation and consistency with direct inversion of Mobius domain-wall Dirac operator (direct MDW) but  $T=330$  MeV, it is not good; we use direct MDW.

# AS index = eta invariant [cf. Yamaguchi's talk]

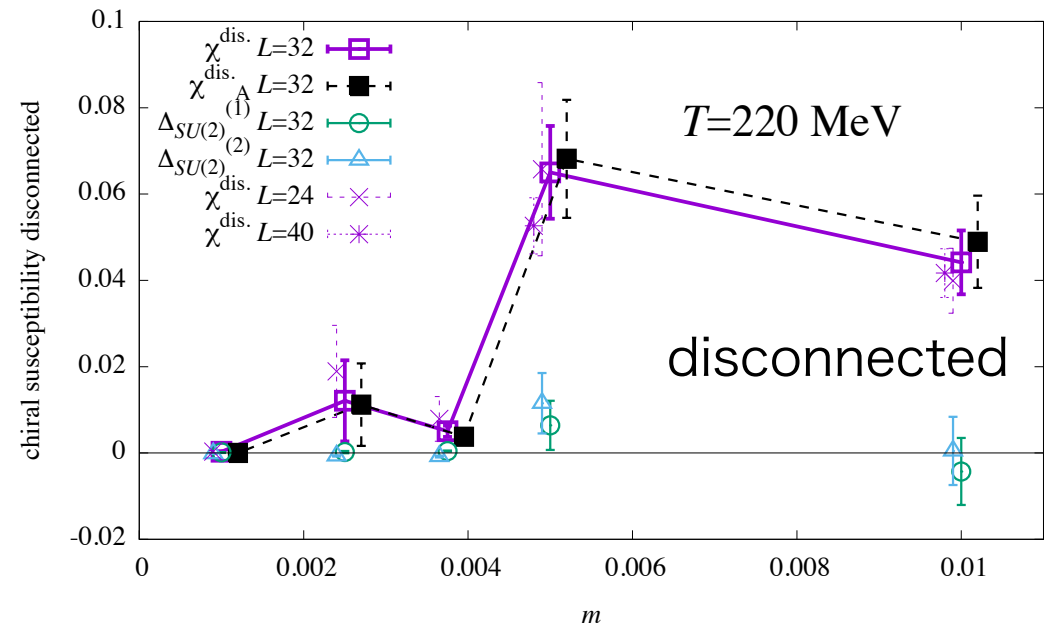
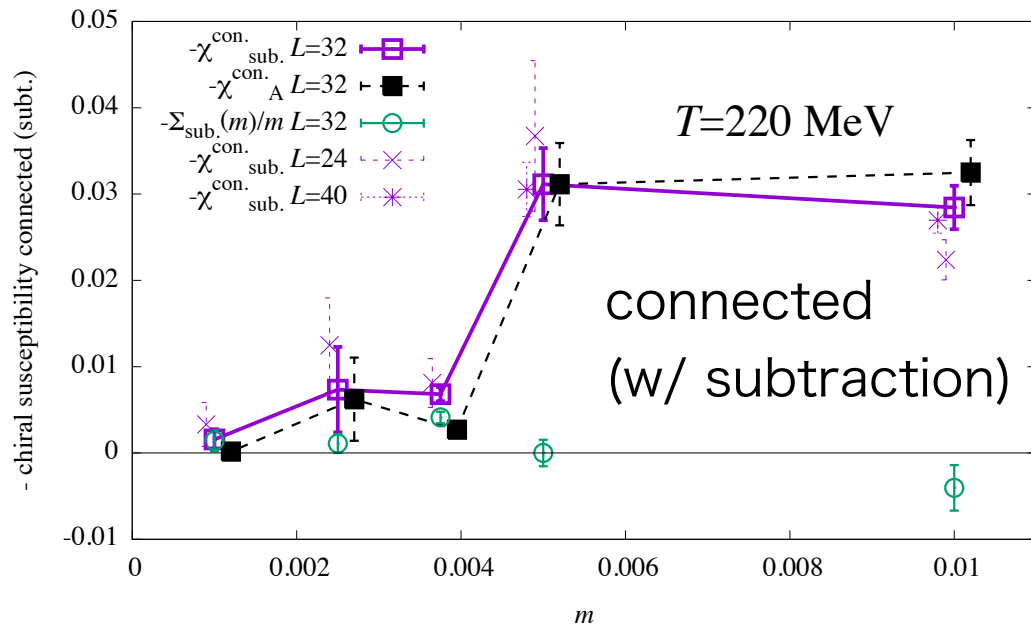
$$\text{Ind}D_{ov} = \eta(\gamma_5(D_{ov} + m))$$

```
data_eigen --zsh-- 80x24
600 -0.005000025807555366 0.302609233991046 1.6064951657562172e-05
600 -0.00500029626669336 0.302609233991046 5.4431872816092406e-05
600 0.005702514532165167 0.302609233991046 0.0027420539675677316
600 -0.005702652525898806 0.302609233991046 0.0027423409419665675
600 0.008534378975613608 0.302609233991046 0.006916416732666278
600 -0.008534900200446262 0.302609233991046 0.0069170598938072675
600 0.0114336277222442 0.302609233991046 0.010282533061119956
600 -0.01143389118468538 0.302609233991046 0.01028282602381281
600 0.01482478910676644 0.302609233991046 0.01395633338456557
600 -0.01482490275384444 0.302609233991046 0.013956454106477945
600 0.01927599474870225 0.302609233991046 0.01861646147547765
600 -0.01927607127753628 0.302609233991046 0.01861654071750083
```

data at beta=4.30, m=0.005, conf=600

Index=-2.

# Nf=2 Result at T=220MeV



Axial U(1) anomaly dominates the signal:

connected part ~ U(1) susceptibility

disconnected ~ topological susceptibility $\times 2/m^2$ .

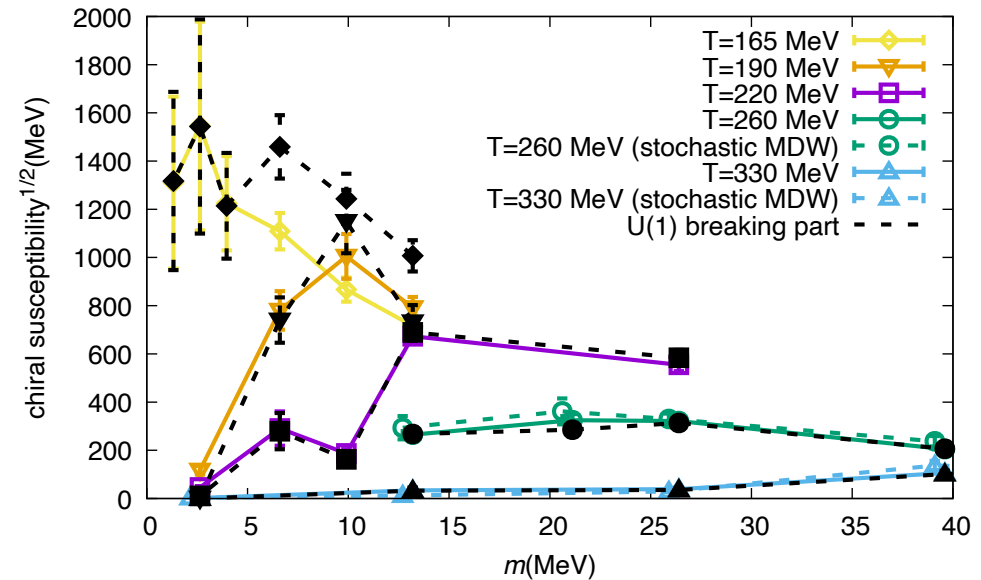
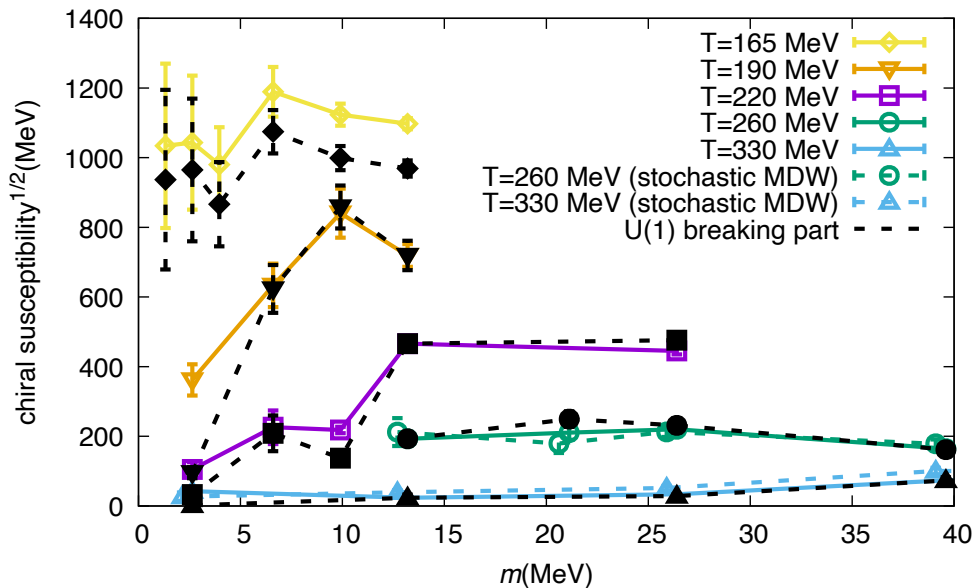
Finite V effects look under control.

Open squares : data for chiral susceptibility

filled squares : axial U(1) anomaly part

crosses and stars : data on different Vs

# Nf=2 at different temperatures



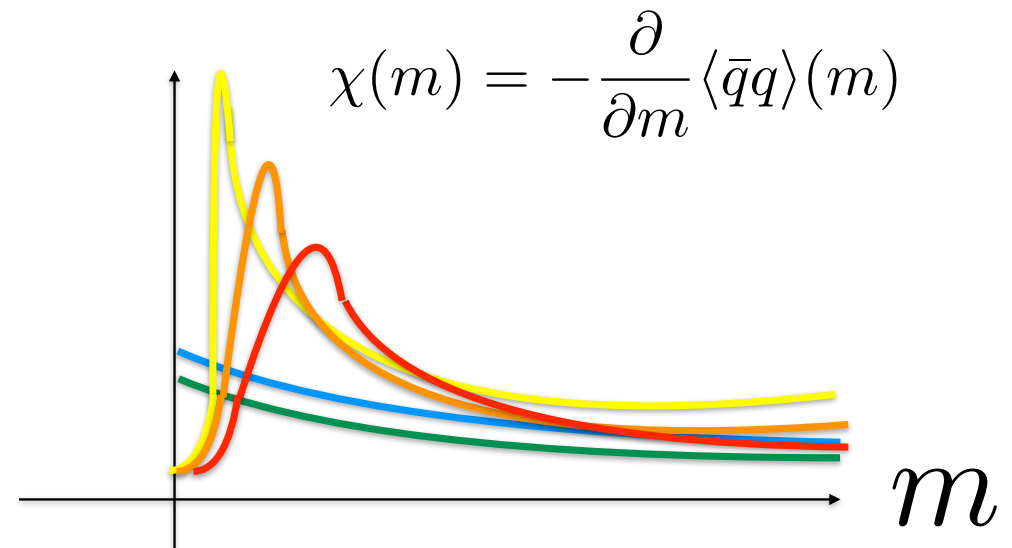
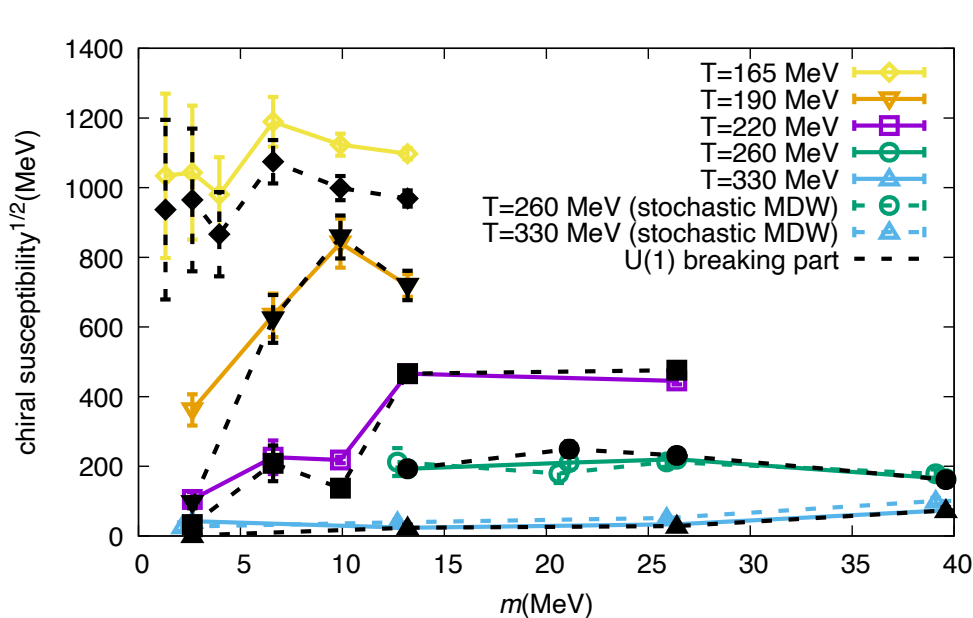
The dominance by axial U(1) anomaly is seen at 5 different Ts.

In fact, ~90% of the signal is from axial U(1) anomaly.

Also note that the chiral limit of anomaly part looks consistent with zero.

**T=165 results are new.**

# Nf=2 at different temperatures



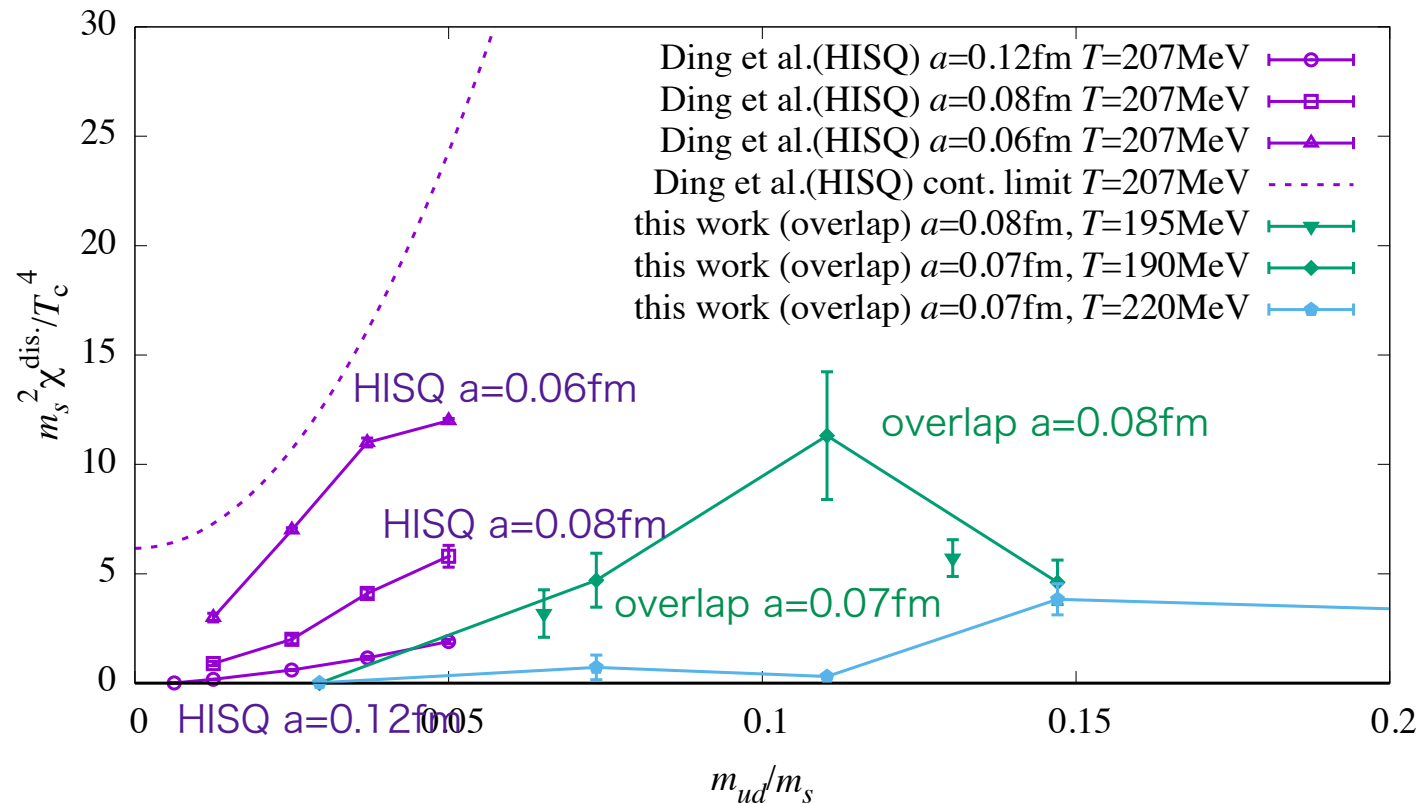
The dominance by axial U(1) anomaly is seen at 5 different Ts.

In fact, ~90% of the signal is from axial U(1) anomaly.

Also note that the chiral limit of anomaly part looks consistent with zero.

T=165MeV results are obtained from OFP/SQUID.

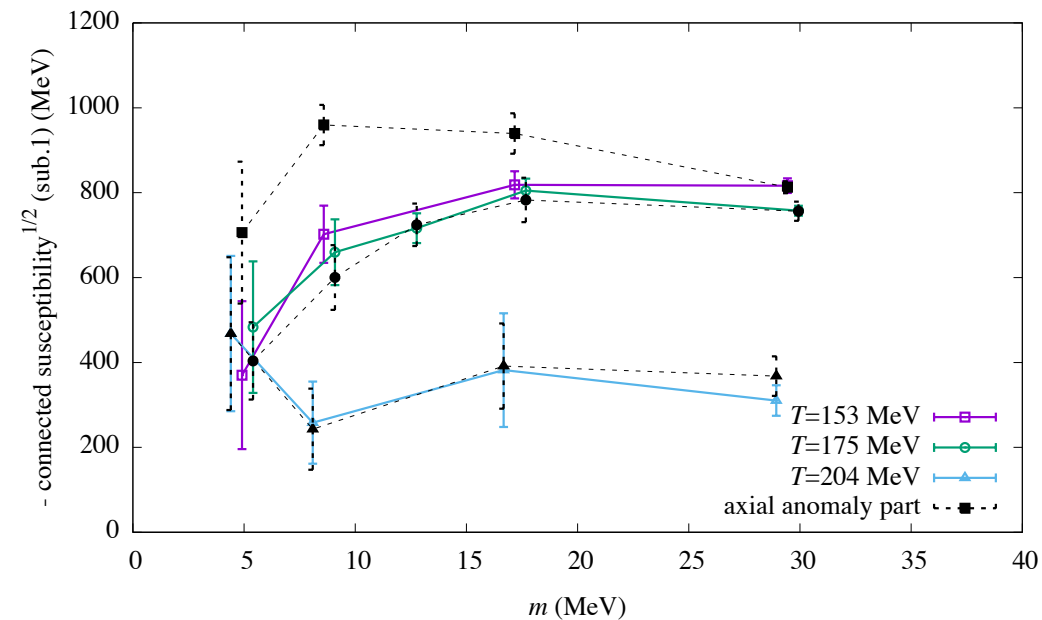
# At different lattice spacings



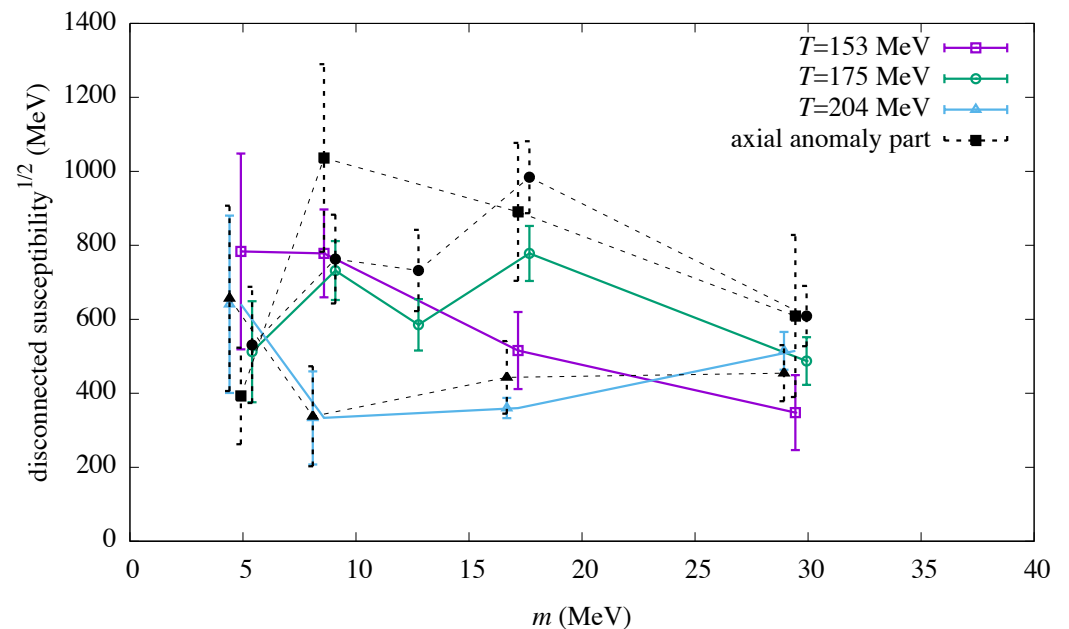
Our data at  $a=0.07\text{fm}$  and  $0.08\text{fm}$  are consistent,  
in contrast to HISQ results [Ding et al. 2020 ]

# Nf=2+1 preliminary results

## connected



## disconnected



The dominance by axial U(1) anomaly is seen at 3 different  $T$ s.  
But the peaks look not significant.

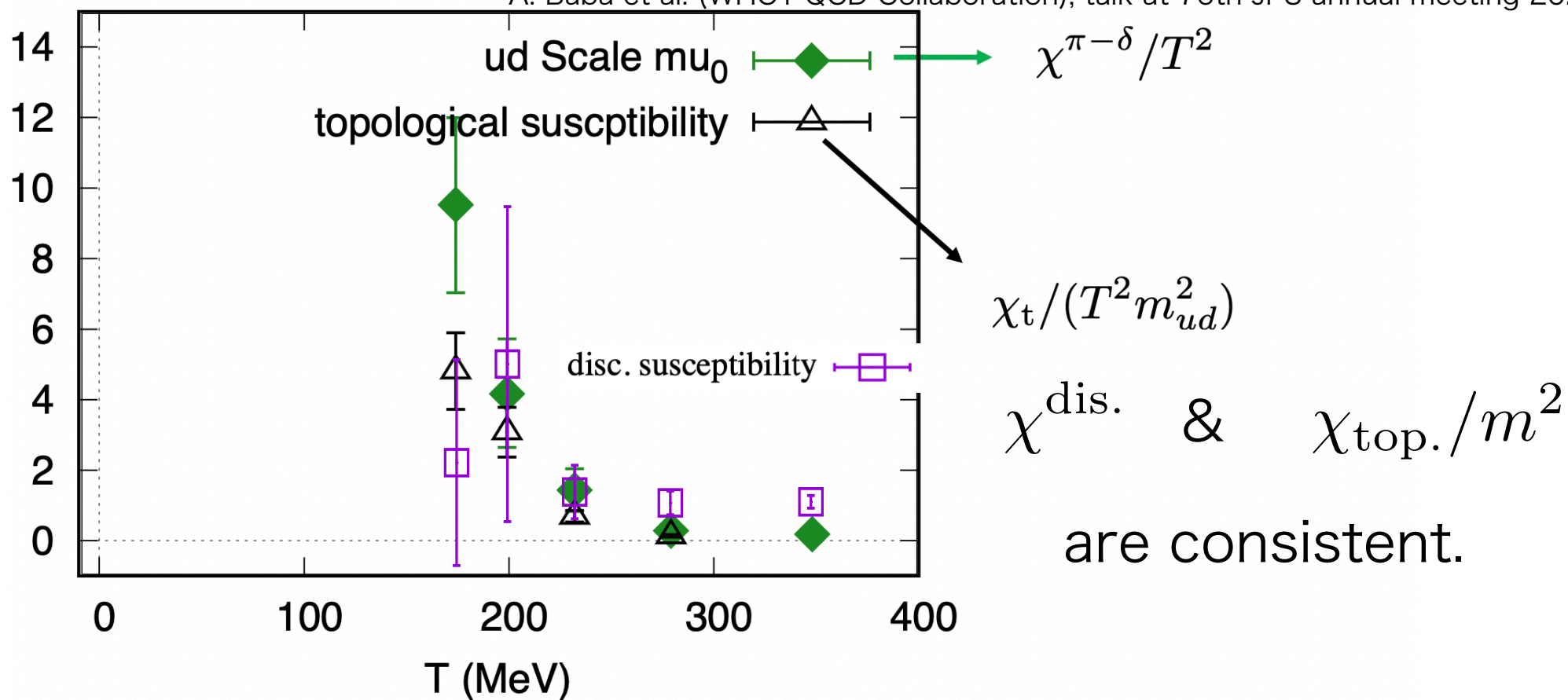


# The same in WHOT-QCD collaboration (?)

We thank A. Baba, S. Ejiri and K.Kanaya for providing us the data.

WHOT-QCD Collaboration, Phys. Rev. D 95, no.5, 054502 (2017)

A. Baba et al. (WHOT-QCD Collaboration), talk at 76th JPS annual meeting 2021



# Subtlety in the total contribution

$$\chi(m) = \chi^{\text{con.}}(m) + \chi^{\text{dis.}}(m)$$

$$\chi^{\text{con.}}(m) = \underbrace{-\Delta_{U(1)}(m)}_{\text{U(1)}_A \text{ breaking contribution}} + \underbrace{\frac{\langle |Q(A)| \rangle}{m^2 V}}_{\text{mixed}} - \underbrace{\frac{\langle \bar{q}q \rangle_{\text{sub.}}(m)}{m}}_{\text{mixed}}$$

$$\chi^{\text{dis.}}(m) = \underbrace{\frac{N_f}{m^2} \chi_{\text{top.}}(m)}_{\text{a large cancellation}} + \underbrace{\Delta_{SU(2)}^{(1)}(m) - \Delta_{SU(2)}^{(2)}(m)}_{\text{SU(2) x SU(2) breaking}}$$

a large cancellation

$O(1/V^{1/2})$  effect

It is difficult to see what survives in the total contribution.

# Contents

## ✓ 1. Introduction

We simulate the chiral phase transition of  $N_f=2$  QCD with chiral fermions to investigate the role of axial  $U(1)$  anomaly.

## ✓ 2. $U(1)_A$ contribution to chiral susceptibility

can be separated using Ward-Takahashi identities.

## ✓ 3. Numerical results

The signal is dominated by axial  $U(1)$  anomaly.

## 4. Summary

# Summary

1. We simulate  $N_f=2$  and  $2+1$  lattice QCD.
2. Chiral condensate/susceptibility are related to both  $SU(2)\times SU(2)$  and  $U(1)_A$ .
3. In the spectral decomposition of the Dirac operator **with exact chiral symmetry**, we can separate the purely  $U(1)$  anomaly effect.
4. **Connected/disconnected susceptibilities are dominated by  $U(1)$  breaking at  $T \geq T_c$ .**

Connected part  $\sim$  axial  $U(1)$  susceptibility.

Disconnected part  $\sim$  top. susceptibility  $\times 2/m^2$

Axial  $U(1)$  anomaly may play more important role in the QCD phase diagram than expected.

## Take-home message

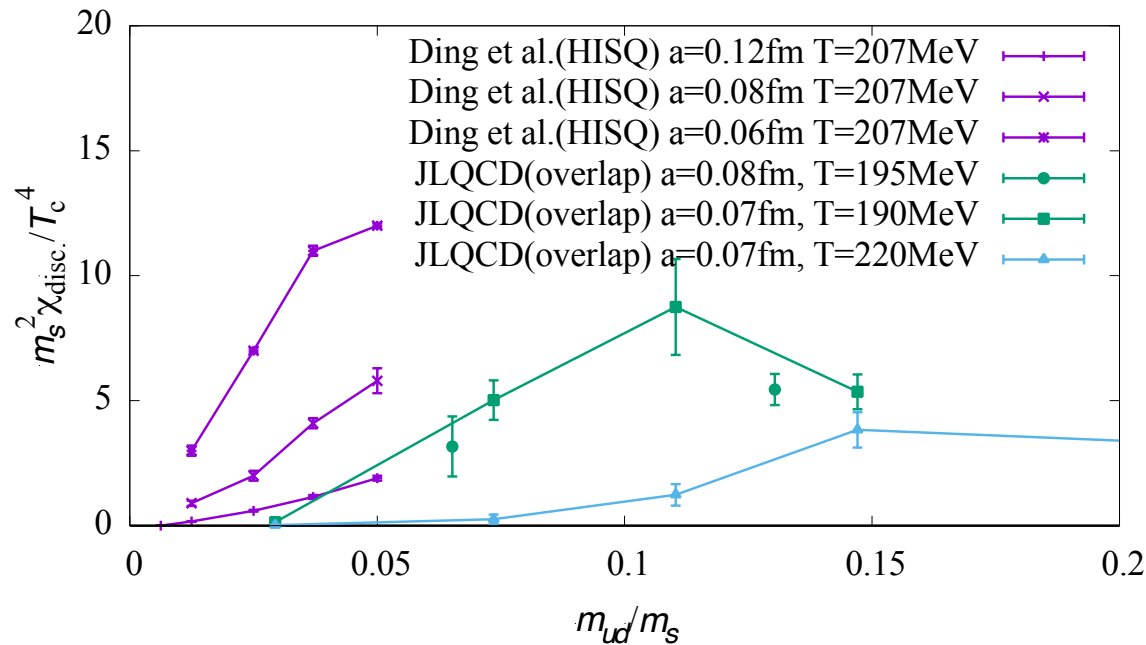
$$\frac{\partial}{\partial m} \langle \bar{\psi} \psi \rangle$$

is probing not only  $SU(2)_L \times SU(2)_R$  but also  $U(1)_A$  breaking/restoration.

At  $T \geq 165 \text{ MeV}$  in  $N_f=2$  QCD ( $\geq 153 \text{ MeV}$  in  $N_f=2+1$ ).

$U(1)_A$  anomaly dominates the signal of connected/disconnected susceptibilities.

# Comparison between Ding et al. 2010.14836 and JLQCD



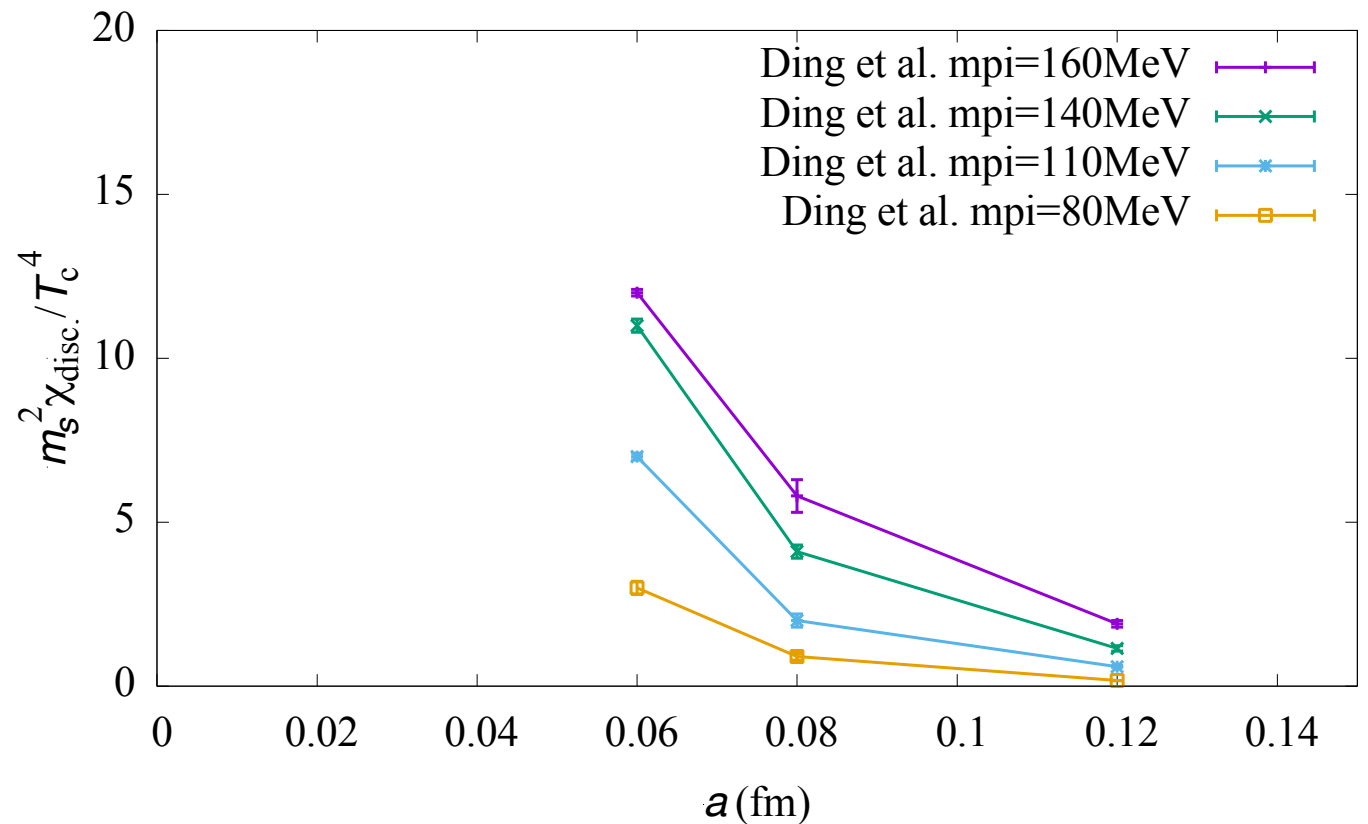
1. Sharp decrease towards the chiral limit is **similar**.
2. Ding et al. shows a **sizable cut-off effect**, while JLQCD's  $a=0.07\text{fm}$  ( $T=190\text{MeV}$ ) and  $0.08\text{fm}$  ( $T=195\text{MeV}$ ) data are consistent.

# Cutoff dependence of Ding et al. 2010.14836

We see a power-like increase.

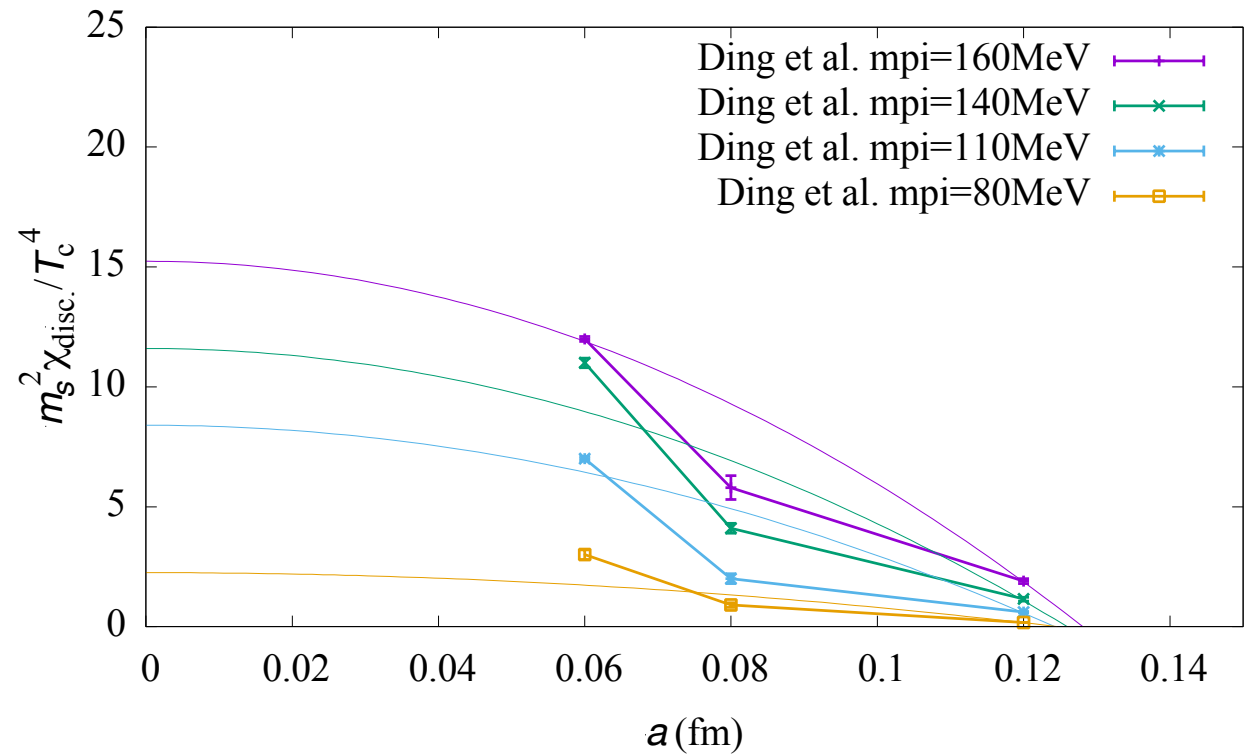
But they managed to obtain “continuum limits”.

How?



# 2-parameter fit clearly fails.

$\chi^2/\text{d.o.f.} > 100.$



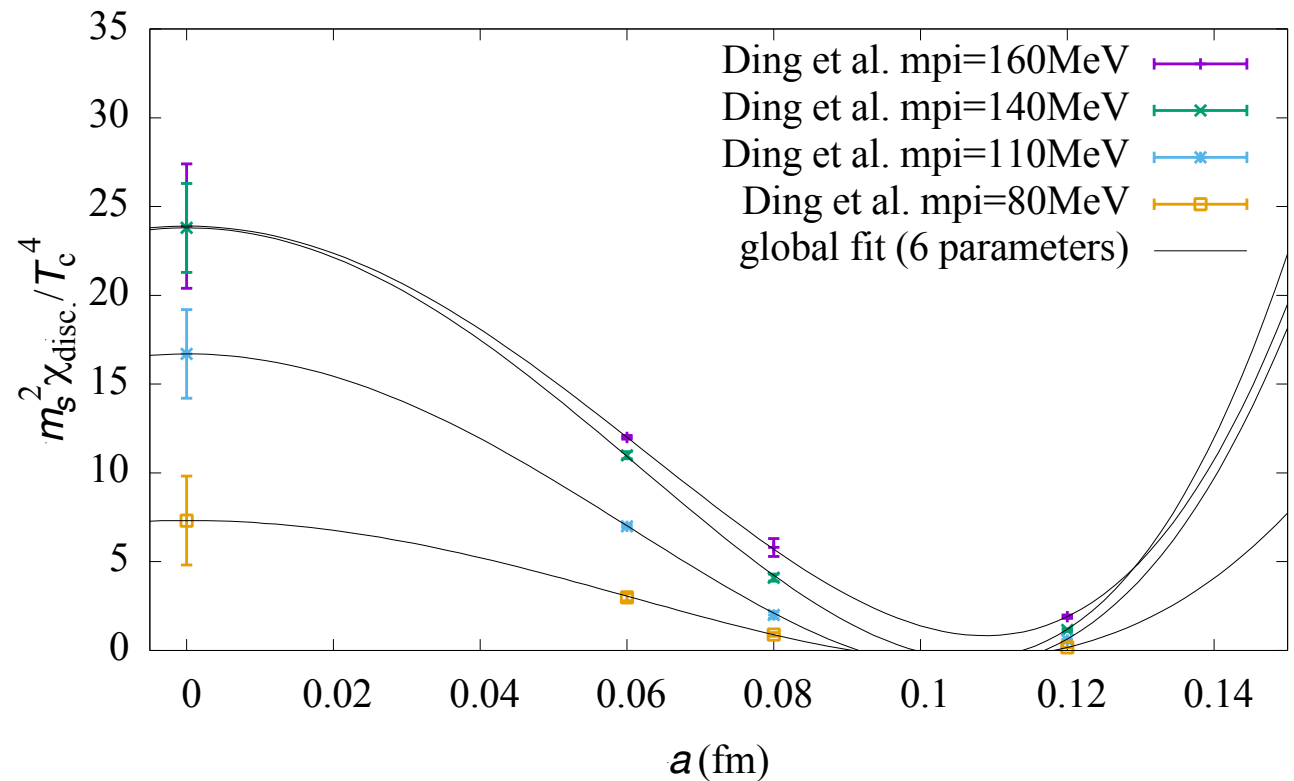


# Global fit “magic”.

More free parameters  
(from 2 to **6**.)

But the fit is **unstable** :  
sensitive to the  
 $O(a^4)$  terms.

Inegative  $O(a^2)$  term  
~ |positive  $O(a^4)$  term|  
already at  $a \sim 0.07$  fm.



# Summary of my comments

1. Sharp decrease towards the chiral limit is **similar to JLQCD's**.
2. But data of Ding et al. 2010.14836 show a power-like increase towards the continuum limit (**due to some lattice artifact?**).
3. By a global fit “magic”, Ding et al. obtained finite values (which are **much bigger than raw values**).
4. But the **6-parameter** fit is unstable : sensitive to  $O(a^4)$  terms.

John von Neumann said

“With **four parameters** I can fit an elephant, and with **five** I can make him wiggle his trunk.”